# Lead-free Two-dimensional Perovskite Solar Cells $Cs_3Fe_2Cl_9$ Using MgO Nanoparticulate Films as Hole Transport Material

**Kawther A. Khalaph[1*] and Aqel Mashot Jafar[2]**

**Abstract**

The present paper concerns with the study of impact of merging ($TiO_2/Cs_3Fe_2Cl_9$/MgO) on FTO using the procedure of drop casting method at temperature (70°C). The structural, optical and morphological characteristics of the (MgO) nanoparticles were described via X-ray diffraction (XRD), UV-Vis Spectrophotometer, and scanning electron microscopy (SEM). The estimated value of the thin films (MgO, and $Cs_3Fe_2Cl_9$) optical energy was (3.87) eV and (4.1) eV, correspondingly. The test results of the current–voltage elucidated that the ultimate power conversion efficiency (PCE) of solar cell was (7.57%), and factor of filling was (54.2). The present research elucidates and investigates the effective hybrid Lead-free Perovskite solar cells.

**Key Words:** Nanoparticles, Lead-free Perovskite, FSEM, PCE.

**DOI Number: 10.14704/nq.2020.18.2.NQ20137** **NeuroQuantology 2020; 18(2):127-132**



## Introduction

Material of high efficiency solar cells absorbs the light above a broad spectral range, creates high efficiency charges, and recharges such created charges to the electrodes with minor losses. [1,2]. Perovskite ($Cs_3Fe_2Cl_9$)from the semiconductors has taken a high deal of consideration owing to its great light absorption making it utilize in the solar cells [3-5].It is one of the members of (A3M2X9)(A(cations)= Cs, Rb; M(cations)= Ti, V, Cr, Fe; X(halogen ion)= Cl, Br, I), possessing interesting magnetic properties [6,7].Recently, the request for the nanostructured substances has raised importantly not only because of the evolution of equipment, but also due to appearance of adapted nanoparticles physical characteristics in comparison with their bulk materials [8]. The semiconductors (MgO) characteristics are non-toxic and cheap; they have taken much attention owing to their potential uses on the solar cells.

The improved solar cell efficiency was the result of a magnesium oxide film, as the broadband gap MgO layer declines the electron transmission to triiodide electrolyte and retards the re-combination of holes and back-transferred electrons [9,10].The current work reveals and investigates the effective hybrid Lead-free perovskite solar cells, as well as studying their materials characteristics.

## Experimental Method

### *Preparation of (MgO) nanoparticles*

MgO NPs were fabricated employing a chemical (precipitation) technique. In a distinctive fabrication process, a (0.1M) of Cu nitrate [$Mg(NO_3)_2.6H_2O$] was solved in 100 mL of distilled water, that has been stirred with a magnetic stirrer for (15) minutes till fully dissolved.

**Corresponding author:** Kawther A. Khalaph
**Address:** [1*]Medical College, IbnSina University of Medical and Pharmaceutical Sciences. Baghdad, Iraq; [2]Solar Energy Research Center, Renewable Energy Directorate, Higher Education and Scientific Research Ministry, Baghdad, Iraq.
[1*]E-mail: kawther75910@gmail.com
**Relevant conflicts of interest/financial disclosures:** The authors declare that the research was conducted in the absence of any commercial or financial relationships that could be construed as a potential conflict of interest.
**Received:** 13 January 2020 **Accepted:** 10 February 2020

(0.2M) from the solution of sodium hydroxide (NaOH) was solved in (100 mL) distilled water, after that, the addition of the combination was donevia dropping it inthe [Mg $(NO_3)_2.6H_2O$] settlement under uninterrupted stirring for 125 minutes and then heating at (65°C). The mixture of reaction developed a white solution and was cleaned thoroughly by distilled water for removing impurities from output[11]. Then, it was dehydrated at (50-75°C) for (1h). Eventually, the sediment was put in an oven that uses hot air at (500°C) for (3h).

### *Preparation of ($Cs_3Fe_2Cl_9$) Via Chemical Reaction*

Perovskite ($Cs_3Fe_2Cl_9$) was produced employing a chemical reaction, to prepare $FeCl_3$ solution, a (0.5g) of powder $FeCl_3$was solved in 10 ml of anhydrous Dimethyl Formamide (DMF), (Sigma Aldrich).For preparing the solution of CsCl, a (0.778g) of powder CsCl was solved in (10 ml)of (DMF) [12]. The perovskite was formed by mixing the $FeCl_3$ solution and the CsCl solution. A previous report showed that to ensure the adequate conversion resistance, a full encasement of perovskite film should be existed on the substrate.

### *PV Device Fabrication*

The planar type PSCs are more classified into a pair of bands arranging: (n–i–p and p–i–n) planar. PSCs consists of an energetic perovskite stratum that is sandwiched among the hole-transporting layer (HTL) and electron-transporting layer (ETL) [13].The $TiO_2$precursor solution was precipitated via the drop casting onto a transparent conductor(FTO)glass during heating, sheet resistance (15 Ω) at (50°C). Next, the solution of perovskite ($Cs_3Fe_2Cl_9$) was deposited via the drop casting on to the pre-heated (FTO/$TiO_2$) substrates at (75°C).The MgO is then poured onto the substrates (FTO/ $TiO_2$/$Cs_3Fe_2Cl_9$)to get the samples of (FTO/$TiO_2$/$Cs_3Fe_2Cl_9$/MgO), and Al foil with a (0.1cm$^2$) area, as an electrode, was placed above theMgO layer, as depicted in figure (1) which shows the structure thin films of Photo-Voltaic (PV) device.

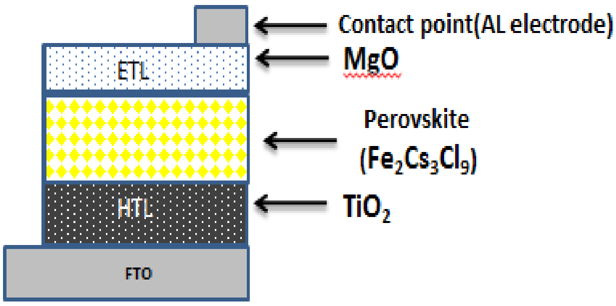


**Fig.1.** Diagram of Photo-Voltaic showing ($TiO_2$/$Cs_3Fe_2Cl_9$/MgO) layer deposited on the FTO

## Results and Discussion

Structural and physical characteristic of ($Cs_3Fe_2Cl_9$, and MgO) was investigated via utilizing the samples characterization via the X-ray diffraction. The surface terrain was detected and configured by (FSEM). Measurements of the optical properties of the light band-gap were found via(UV-VIS)Spectrophotometer.

### *X-Ray Diffraction Measurement*

The (XRD) patterns of synthesized (MgO,$Cs_3Fe_2Cl_9$) crystalline nature are shown in figure (2). In such figure, it can be observed that these patterns correspond to the powders (MgO,$Cs_3Fe_2Cl_9$) value as compared toJCPDS No. 89-2531 and JCPDS No. 07-0235 as well asJCPDS No. 36-1451, correspondingly. The patterns results of the XRD are reflected in the fact that the expansion of diffraction peaks manifests the existence of (MgO)nanostructureand($Cs_3Fe_2Cl_9$)via applying equation (1), which is the Debye-Scherrer expression[11,14]:

$$D = \frac{0.9\lambda}{\beta\cos\theta} \ldots\ldots\ldots (1)$$

Where:
D: Crystalline size
λ: X-ray wavelength (1.5406˚A)
θ: Diffraction peakdegree
β: Full peak width at half maximum (FWHM)

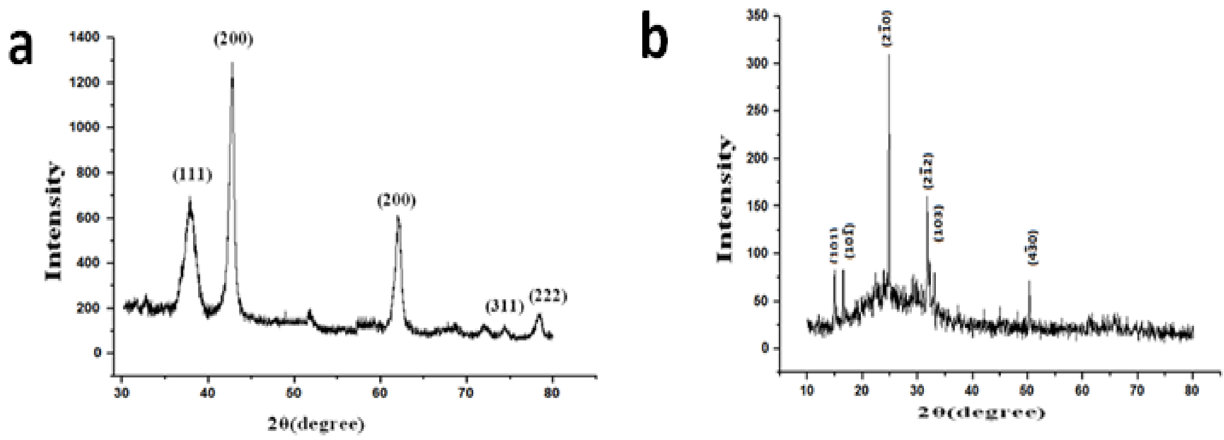


**Fig. 2.** The X-ray diffraction patterns of (a) MgOand (b)$Cs_3Fe_2Cl_9$

The crystalline size of (MgO) elucidates that the arranged samples sizes were within the nanoscale, as revealed in the Table (1).

**Table 1.** Values of 2θ, FWHM, d-value and sizeof crystalline

| Sample | (2θ), (deg.) | (FWHM), (deg.) | (d-value), (A°) | Size of crystalline, (nm) |
|---|---|---|---|---|
| MgO | 37.71 | 0.89 | 2.38 | 9.45 |
| | 42.72 | 0.58 | 2.11 | 14.74 |
| | 61.95 | 0.69 | 1.49 | 13.45 |
| | 74.27 | 0.50 | 1.27 | 19.95 |
| | 78.3 | 0.69 | 1.21 | 14.86 |
| $Cs_3Fe_2Cl_9$ | 16.59 | 0.13 | 5.33 | 61.91 |
| | 24.84 | 0.17 | 3.58 | 47.97 |
| | 31.80 | 0.17 | 2.81 | 48.70 |

## *FESEM of MgO and Perovskite ($Cs_3Fe_2Cl_9$)*

The (FSEM) images of the thin-film nanostructures as arranged (MgO, and $Cs_3Fe_2Cl_9$) with two various enlargements. Figures 3 (a,b) depicts that the (MgO) nanoparticles constitution was almost spherical, and the perovskite was almost parallel rectangles.



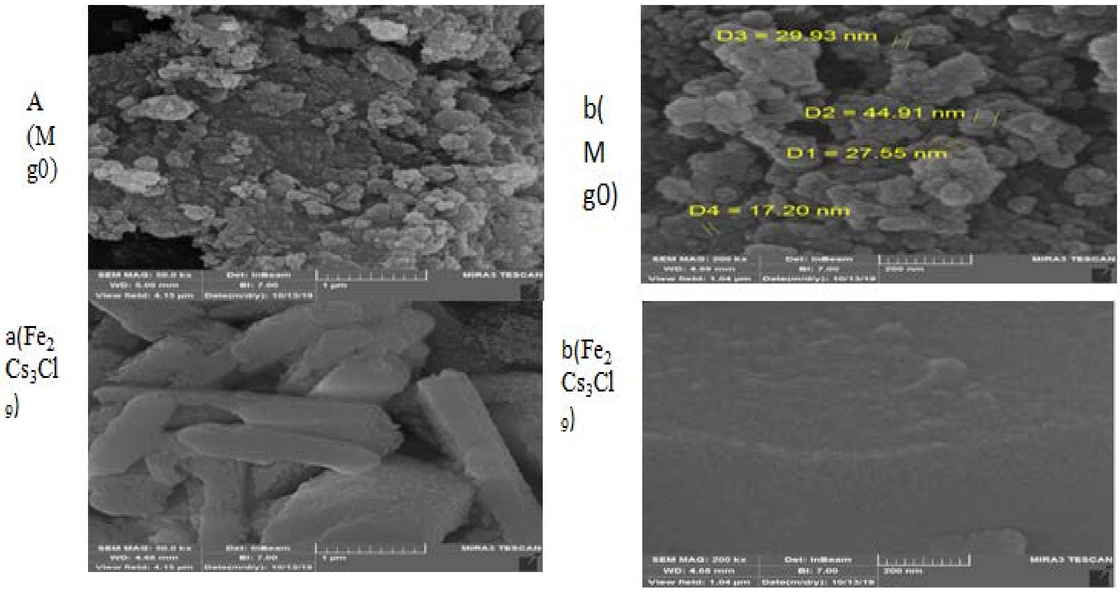


**Fig. 3.** (a,b) The (FESEM) images measurement (1 μm, 200 nm), respectively

### *Optical Properties*

Figure (4a) depicts the optical absorption of ($Cs_3Fe_2Cl_9$andMgO) films measured by using the (UV-VIS)in a range of wavelength (200-1100 nm). From peak spectra or shoulder, the samples absorption edges can be utilized for estimating the gap via the extrapolation of the curve' s linear part [11]. The band gap of energy was computed by equation (2)[15]:

$$(\alpha h\upsilon) = B^* (h\upsilon\text{-}Eg)^n \ldots\ldots\ldots (2)$$

Where,
α: The coefficient of absorbance
h: Constant of Plank
B: Experimental constant
ν:Light frequency
n:A constant that relies upon transmission either (1/2) for direct.
Eg: The energy band gap.

Figure (4b) illustrates the band-gap of (MgO) NPsand ($Cs_3Fe_2Cl_9$).The band-gap estimated value for (MgO and $Cs_3Fe_2Cl_9$) was (4.05and 2.5eV), respectively, as shown in figure (4b)[11]. The sample thickness was corroborated as a significant parameter to estimate (Eg),it was measured ($t_{MgO}$ = 148.5nm, and $t_{Cs3Fe2Cl9}$=400nm to 600 nm). The quantum limitation influences the band-gap energies increment in (MgO) nanostructures owing to the size reduction of structures. Such outcomes relate to the those of the XRD and the FESEM.

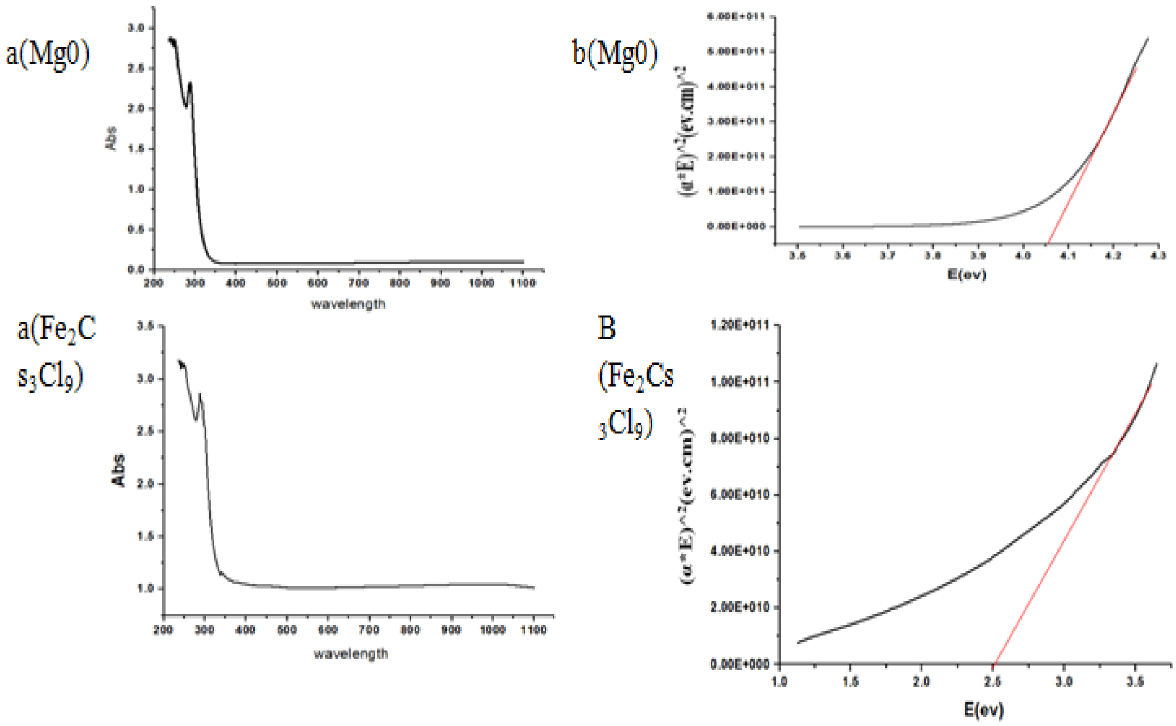


**Fig.4.** (a) The visual absorption and (b) the films energy gap(Eg)



### *Hall Effect*

The Hall effect is one of the most important ways to study the electronic properties of solids, especially semiconductors. One of the most common and interesting measurements in thin-film applications is the information it provides about the nature of the sample examined, whether they have a negative electrical conductivity (n-type) or a positive (p-type) through the Hall coefficient signal (RH), as well as giving accurate data on the concentration and movement of charge carriers in them [16]. For moderate magnetic fields, the Hall coefficient is:

RH = (Pμ-h2-nμ-e2) / (pμ-h+nμ-e)2 ……… (3)

Figure (5) illustrates thehall effect of MgOpositive (p-type).

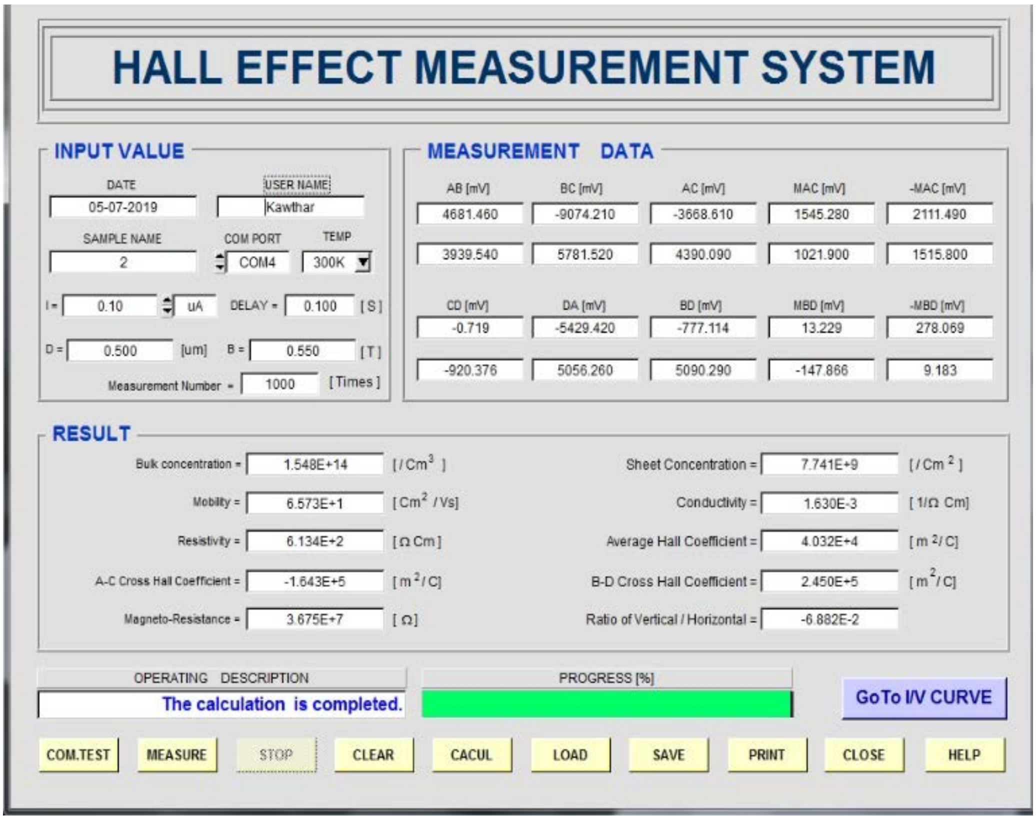


**Fig.5.** Hall effect of MgO

## *Power Conversion Efficiency (PCE) Measurement*

Figure (6) demonstrates the properties (PCE) of ($TiO_2/Cs_3Fe_2Cl_9/MgO$), Fill Factor, short circuit current, efficiency, and open circuit voltage.

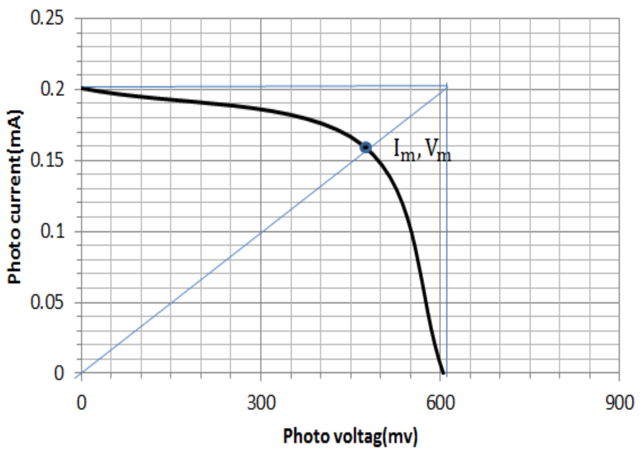


**Fig. 6.** The (I-V) curve of the Perovskite solar cell

High efficiency can be obtained using ($TiO_2$,$Cs_3Fe_2Cl_9$andMgO).For the solar cell,the fill factor (F.F.)and the power conversion efficiency (PCE)were computed by equations (4) and (5), respectively[15]:

$$F.F. = \frac{I_m V_m}{I_{sc} V_{oc}} = \frac{P_m}{I_{sc} V_{oc}} \quad \ldots\ldots\ldots (4)$$

$$\mathbf{PCE} = \frac{V_{OC} \cdot I_{SC} \cdot FF / A_{SC}}{P_{in}\ mw/cm^2} \ldots\ldots\ldots\ldots (5)$$

Where,

F.F.: The fill factor, $V_{OC}$: The open circuit voltage, $I_{SC}$: The short circuit current

Theses parameters can be found at the room temperature, and they possess the values (54.2, 269.8 mV, and 0.16 mA), correspondingly. The Perovskite solar cell efficiency (PCE) is 7.57%.



## Conclusions

In the present investigation, a Perovskite solar cell was effectively produced. Results evinced that the arranged (MgO) materials descriptions being nanostructures utilized to improve solar cell efficiency. MgO is proper hole extractor, HTL, where as the $TiO_2$ is employed for extracting proper electrons, ETL. From energy efficiency conversion (PCE) results, it was noticed that solar cell photovoltaic characteristics were enhanced utilizing MgO NPs.

## References

Belous A, Kobylianska S, V'yunov O, Torchyniuk P, Yukhymchuk V, Hreshchuk O. Effect of non-stoichiometry of initial reagents on morphological and structural properties of perovskites CH3NH3PbI3. Nanoscale Res. Lett., 2019; 14(1).

Khalaph KA, Shanan ZJ, Al-Attar FM, Abd AN, Jafar AM. Fabrication and investigation of hybrid Perovskite solar cells based on porous silicon. Materials Today: Proceedings 2020; 20: 605-610.

Chen LC, Weng CY. Optoelectronic properties of MAPbI 3 perovskite/titanium dioxide heterostructures on porous silicon substrates for cyan sensor applications. Nanoscale research letters 2015; 10(1): 1-5.

Im JH, Chung J, Kim SJ, Park N. Synthesis, structure, and photovoltaic property of a nanocrystalline 2H perovskite-type novel sensitizer (CH3CH2NH3)PbI3. Nanoscale Res. Lett., 2012; 7(1).

Hamatani T, Shirahata Y, Ohishi Y, Fukaya M, Oku T. Arsenic and Chlorine Co-Doping to CH3NH3PbI3 Perovskite Solar Cells. Adv. Mater. Phys. Chem., 2017; 7(1): 1–10.

Hagihala M, Masuda T. Magnetic structure of S=5/2 spin-dimer compound Cs3Fe2Cl9 2018.

Wei F, Brivio F, Wu Y, Sun S. Bristowe PD, Cheetham AK. Synthesis, crystal structure, magnetic and electronic properties of the caesium-based transition metal halide Cs3Fe2Br9. J. Mater. Chem. C, 2018; 6(14): 3573–3577.

Granitzer P, Rumpf K, Ohta T, Koshida N, Poelt P, Reissner M. Porous silicon/Ni composites of high coercivity due to magnetic field-assisted etching. Nanoscale Res. Lett., 2012; 7(1).

Photiphitak C, Rakkwamsuk P, Muthitamongkol P, Thanachayanont C. Performance Enhancement of Dye-Sensitized Solar Cells by MgO Coating on TiO2 Electrodes 2012; 6(5): 485–489.

Jung HS. Preparation of nanoporous MgO-coated TiO 2 nanoparticles and their application to the electrode of dye-sensitized solar cells. Langmuir 2005; 21(23): 10332–10335.

Somanathan T, Krishna VM, Saravanan V, Kumar R, Kumar R. MgO nanoparticles for effective uptake and release of doxorubicin drug: PH sensitive controlled drug release. J. Nanosci. Nanotechnol., 2016; 16(9): 9421–9431.

Karuppuswamy P. Role of a hydrophobic scaffold in controlling the crystallization of methylammonium antimony iodide for efficient lead-free perovskite solar cells. Nano Energy, 2017; 45: 330–336.

Wang R, Mujahid M, Duan Y, Wang ZK, Xue J, Yang Y. A Review of Perovskites Solar Cell Stability. Advanced Functional Materials 2019.

Chen LC. Nano-structured CuO-Cu2O Complex Thin Film for Application in CH3NH3PbI3Perovskite Solar Cells. Nanoscale Res. Lett., 2016; 11(1).

Suhail MH, Jafar AM. Fabrication and Characterization of Organolead Halide Peroviske Solar. In Elixir Renewable Energy 2016; 98: 42709–42713.

Etgar L. Hole Conductor Free Perovskite-based Solar Cells. Cham: Springer International Publishing 2016.